Appl. Phys. B 53, 339–346 (1991)

Applied Physics B Photophysics and Laser Chemistry

The Application of Single-Pulse CARS for Temperature Measurements in a Turbulent Stagnation Flame

W. Meier, I. Plath, and W. Stricker

DLR-Institut für Physikalische Chemie der Verbrennung, Pfaffenwaldring 38, W-7000 Stuttgart 80, Fed. Rep. Germany

Received 8 July 1991/Accepted 27 August 1991

Abstract. N_2 Q-branch CARS spectra have been recorded and evaluated for temperature determination in a turbulent, premixed CH_4/air stagnation flame with a burner of 40 mm diameter and 22 kW thermal load. Temperature histograms on the flame axis at different distances from the stagnation plate have been measured. Problems of practical applicability are addressed, including those arising from the limited spatial resolution of the BOXCARS geometry, from an insufficient dynamic range of the diode array detector, and from a memory effect of the detector in the case of measurements in highly turbulent flame areas with strong intermittency. Some information is given on the computerized acquisition and on the evaluation of the large amounts of data that are necessary for extensive investigations in large combustion systems.

PACS: 33.20, 42.65

CARS (coherent anti-Stokes Raman scattering) is one of the most promising techniques for non-intrusive temperature measurements in the hostile environment of a flame. Employing a broadband excitation scheme, single-pulse measurements can be performed to yield instantaneous temperature values, and from these, probability density functions of the temperature can be derived. For combustion thermometry the broadband CARS technique offers several advantages: good spatial and temporal resolution; high measurement precision; and strong signal intensities in a directed laser-like beam. Accordingly, the applicability of this method to single shot thermometry has been demonstrated in many experiments (e.g. [1]). The special properties of the CARS technique suggest that it should also be an ideal tool for the investigation of turbulent flames. However, recent studies have shown that difficulties arise from the extreme inhomogeneities in turbulent flame zones [1–4]. Steep density gradients result in optical perturbations and signal loss because of beam degradation or distortion of the beam overlap. Large temperature fluctuations in turbulent flame fronts lead to changes in CARS signal intensities of more than three orders of magnitude exceeding the dynamic range of commonly used detectors. The small spatial structure of the turbulent flame front cannot always be resolved properly, even if a crossed beam BOXCARS geometry is employed.

In this paper, single-pulse CARS temperature measurements in a turbulent stagnation flame are presented, along with details addressing most of the different problems associated with CARS thermometry in turbulent flames. These problems are discussed in detail and solutions with respect to practical applications are given.

1 Theory

Several reviews include a detailed treatment of the CARS theory [5–7], therefore, only a brief summary will be given here. Incident laser beams at frequencies ω_1 and ω_2 ($\omega_1 > \omega_2$, called pump and Stokes beam, respectively) interact through the third-order non-linear susceptibility $\chi^{(3)}$ of the medium to generate an oscillating polarization, which acts as the source of coherent radiation at frequency $\omega_3 = 2\omega_1 - \omega_2$. A resonant enhancement of the CARS radiation is achieved when the frequency difference $\omega_1 - \omega_2$ is equal to a Raman active transition frequency ω_R of the molecules in the medium. The CARS intensity is given by [5]

$$I_{\mathrm{CARS}} \propto \omega_3^2 I_1^2 I_2 |3\chi^{(3)}|^2 L^2 F(\Delta k \cdot L), \tag{1}$$

where I_1, I_2 are the intensities of the pump and Stokes beam, L is the interaction length, $\chi^{(3)}$ is the third-order

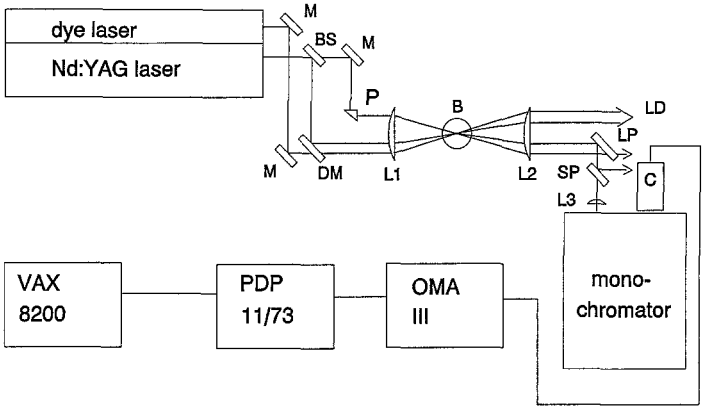

Fig. 1. Experimental setup. M: mirror; BS: beam splitter; P: prism; DM: dichroic mirror; L: lens; B: burner; LD: laser dump; LP, SP: optical filter; C: camera

non-linear dielectric susceptibility and $F(\Delta k \cdot L)$ is the phase matching function. $\chi^{(3)}$ can be expressed as

$$\chi^{(3)} \propto \sum_{v,J} \Delta N \frac{\omega_R}{\omega_R^2 - (\omega_1 - \omega_2)^2 - i\Gamma \cdot (\omega_1 - \omega_2)} + \chi_{NR}, \qquad (2)$$

where ΔN is the difference in population between the lower and upper state for a particular transition, Γ is the damping constant (homogeneous Raman linewidth) and χ_{NR} is the nonresonant susceptibility. $\chi^{(3)}$, and therefore also I_{CARS}, varies with $(\omega_1 - \omega_2)$ leading to a characteristic CARS spectrum for each molecular species (with Raman resonances ω_R). The temperature information is included in the population difference and can be unambiguously deduced from the intensity distribution within the spectrum. In combustion thermometry with CARS, it is most common to use the Q-branch spectrum (transition rule $\Delta v = 1$, $\Delta J = 0$) of molecular nitrogen.

In contrast to scanning CARS, where $(\omega_1 - \omega_2)$ is tuned over the Raman resonances of the different rotational states, the broadband CARS technique uses a spectrally broad (pulsed) laser source for ω_2, which covers all the Raman resonances ω_R simultaneously. The advantage of this method is that a complete CARS spectrum is generated by each laser pulse, which forms the basis for single shot temperature measurements.

2 Experimental Setup

2.1 Optical Arrangement and CARS Instrument

The experimental setup is schematically shown in Fig. 1. A frequency doubled Nd:YAG laser (JK Laser HY 750, $\lambda = 532$ nm, pulse duration 10 ns) with a repetition rate of 10 Hz was used to deliver the pump frequency ω_1 for the CARS process and, simultaneously, to pump a dye laser for generating the Stokes frequency ω_2. The dye laser was operated with Rhodamin 101 in the oscillator cell and Rhodamin B in the amplifier cell. No wavelength selecting device was used in the resonator. In this way the spectral profile of the dye laser was solely determined by the gain characteristics and the concentrations of the dyes, and resulted in a centre wavelength of about 607 nm with a half-width FWHM of $\approx 120\,cm^{-1}$, according to the wavelength region for the N_2 Q-branch CARS spectrum. The 532 nm laser beam was divided by a 50% beam splitter in order to get two pump beams at ω_1. Both pump waves and the Stokes wave were focused by a plano convex lens ($f = 300$ mm) into the measuring volume within the flame. We applied a planar BOXCARS geometry [5] with an overlap volume of the laser beams of about 2 mm in length and 0.15 mm in diameter. Relatively large focus diameters were chosen in order to avoid saturation effects. The N_2 CARS signal was collimated by a second lens of the same focal length, and, after separation from the laser beams, focused onto the entrance slit of a double monochromator (Spex 1403, 1800 l/mm). The signal intensity could be variably attenuated to fit the dynamic range of the detector. Due to (1), I_{CARS} depends on the product $I_1^2 I_2$ of the laser intensities, which could be changed by a combination of $\lambda/2$ waveplates and polarizers to achieve the desired CARS signal intensity.

2.2 Diode Array Detector

The CARS spectrum was imaged onto a linear, MCP intensified photodiode array camera (EG&G, PAR model 1421). Only 300 out of 1024 diodes were actually used to record a complete N_2 CARS spectrum. To reduce the amount of data, we took advantage of the "grouping mode" of the detector, and added the signals of two adjacent diodes resulting in 150 camera channels for one spectrum.

After each laser pulse the data was transferred to the memory device of the camera controller for transient storage, and, after a detection cycle of typically 500 pulses, passed on to a PDP 11/73 computer (Digital Equipment) for final storage. As an alternative to this mode of operation, the accumulation of many spectra on the diode array was also possible.

Since the construction and operating principle of the intensified camera is of importance to our measurements and data analysis, a more detailed description of the device follows. The photons of the signal beam are converted by a photo cathode to electrons, which in turn are amplified by a microchannel plate. A phosphor screen reconverts the electrons to photons, which are then detected by the photodiodes. Finally, a 14-bit AD-converter provides the digital form of the signal. Three points should be noted here: (1) The detector has a limited range of 16383 counts per pixel at maximum; (2) The intensifier can be damaged when signals exceed the level of about 32000 counts per pixel; (3) The intensifier exhibits afterglow effects, which are probably due to an image persistence of the phosphor screen [8]. The consequences of these effects will be discussed in Sect. 5.

2.3 Burner

The burner with stagnation plate was especially constructed and designed for complementary investigations of turbulent flame characteristics [9]. A particular-

ly important feature is that the flow velocity is perpendicular to the flame front over a wide range of the flame diameter. Figure 2 shows a schematic drawing of the burner. A stoichiometric methane/air mixture (2 m^3/h CH_4, 19.05 m^3/h air) flows out of the converging burner nozzle (i.d. 40 mm) with an average gas velocity of 4.6 m/s. A perforated turbulence grid (obstruction ratio 0.5) is placed inside the tube, 40 mm beneath the rim. The flow is stagnated at a water cooled stainless steel plate 100 mm above the tube, and a stagnation point is built at the centre of the plate. Approaching this stagnation point, the axial flow velocity decreases steadily until it is equal to the local turbulent flame velocity. In this region, a few millimetres below the plate, the flame is stabilized and forms a flat turbulent flame front. Coflowing air from an annular nozzle (i.d. = 54 mm, o.d. = 124 mm) is used to stabilize the rectangular velocity profile, and to protect the flame against external influences. Under our operating conditions the thermal load of the flame was 22 kW.

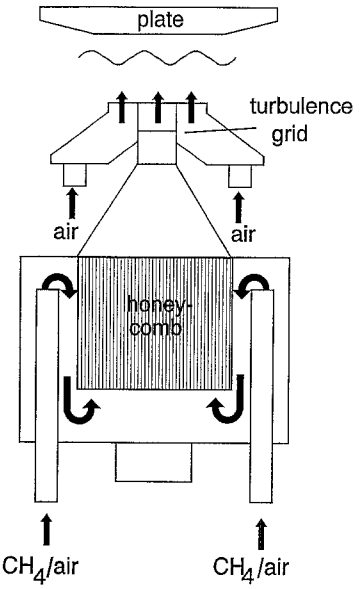

Fig. 2. Schematic drawing of the burner for the stabilization of turbulent stagnation flames

3 Data Collection and Analysis

At each measuring position we recorded between 500 and 1000 single pulse CARS spectra. Prior to computing the temperature values, several corrections had to be performed: signal background subtraction; ratioing with the spectral intensity distribution of the dye laser; and the correction for the detector non-linearities [8, 10, 11]. These procedures are briefly described in the following section.

After each cycle of single shot measurements, the background signal, consisting of dark current and signal offset of the camera, was measured and stored for subtraction. The dye laser intensity varied by about 25% over the spectral range of the N_2 CARS spectrum, and also exhibited shot-to-shot fluctuations. Our equipment did not enable recording of every single pulse dye laser profile, so instead an average dye curve was measured from time to time. For this purpose, a non-resonant CARS signal was generated in CO_2 or argon, reflecting the desired intensity distribution. A notable advantage of this method is that it also corrects for the different sensitivities of the camera pixels. Non-linearities of intensified cameras can lead to temperature errors of 3–6% [8]. The gain characteristics of our camera were thoroughly determined and the corrections added to the data processing program.

There are several ways to derive the temperature from a CARS spectrum and the most common methods are least squares fits of the whole spectral shape, library based fits and quickfitters. A least squares fit compares a calculated spectrum with an experimental one by optimizing parameters like temperature, gas concentration, wavelength position of the spectrum on the diode array or value of the non-resonant background. Library routines are based on pre-calculated spectra which are stored in a library [12–14]. The analysis of an experimental spectrum is performed by finding the best agreement with a library spectrum by interpolation. In this way the temperature and, depending on the program, other parameters can be determined. Quickfit methods are based on temperature dependent characteristics of CARS spectra like halfwidth, quarter-width, area ratios or mean values [15–17].

The data processing time depends strongly on the evaluation method, and for measurements comprising of 10000 single pulse spectra or more necessary for systematic flame investigations, only quickfit methods are of practical importance. A drawback of these methods is that in some temperature intervals they are less accurate than least squares approximations. The temperature accuracy of 23 quickfit methods was determined in a well controlled isothermal furnace and compared with other fit methods. From the results of these investigations, the accuracy of the different quickfit methods could be quantitatively assessed and increased, thus allowing the quality of the current temperature evaluation routines to be improved [16].

The first step of the quickfit methods consists of the calculation of a set of N_2 Q-branch spectra in the temperature range of interest in intervals of typically 50 K. The influence of the experimental conditions on the shape of the theoretical spectra is taken into account by measuring the "instrument transfer function" and convoluting the theoretical spectra with it. From the set of calculated CARS spectra, the values for the halfwidth, area ratios and the other temperature sensitive parameters were extracted, in order to set up a temperature curve for each parameter. In the next step the computer program determined the measured values for these parameters from the experimental spectra, and calculated the temperatures by looking up in the theoretical temperature curve. By this procedure the VAX 8200 computer could deliver more than 20 different quickfit temperature values for each spectrum in less than one second.

Some further options were added to the program to assess the quality of a single pulse CARS spectrum, and to

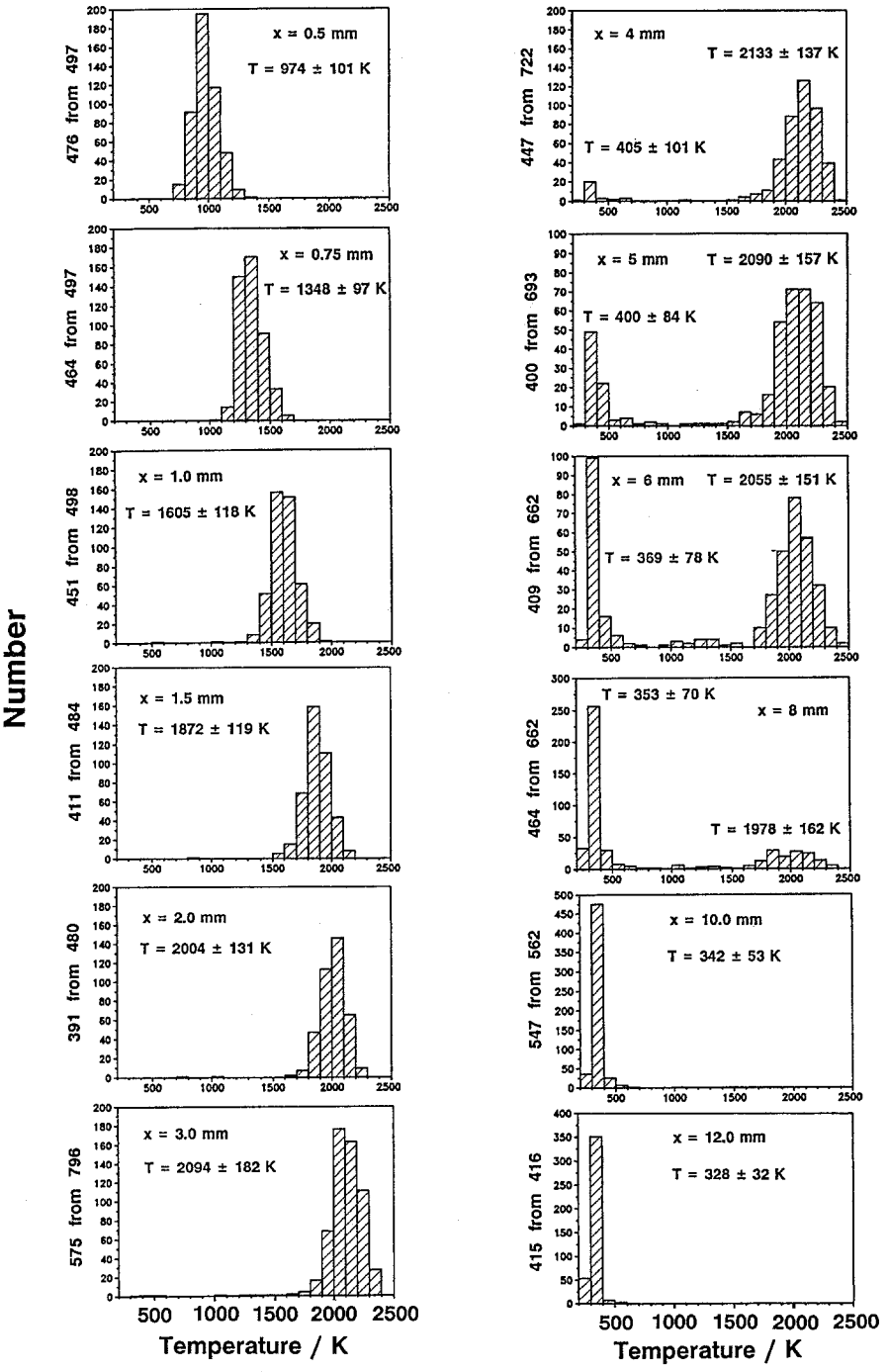

Fig. 3. Temperature histograms measured on the flame axis at distances x from the stagnation plate

withdraw automatically spectra of low quality. This will be discussed in more detail in Sect. 5.

4 Results

At 13 different locations on the flame axis we determined the temperature distributions by recording between 500 and 1000 single pulse CARS spectra at each position. From these spectra, temperature histograms were constructed as shown in Fig. 3. The histograms are ordered according to the distance x from the stagnation plate. The mean temperatures and the standard deviations are specified for each distribution.

Beneath the flame front at distances of 12 and 10 mm from the stagnation plate, the unburnt gas temperature is observed, which is slightly raised by the hot environment. The beginning of the reaction zone is recognizable by the appearance of a few high temperature values at $x=8$ mm. Further downstream the number of spectra showing high temperatures increases, and the proportion showing low temperatures becomes less, eventually disappearing completely at $x=3$ mm. Approaching the cold stagnation plate, the temperature of the exhaust gas decreases steadily, and at $x=0.5$ mm the mean temperature reaches a value of about 1000 K. From these distributions it is clearly seen that the turbulent flame front is characterized by bimodel temperature distributions.

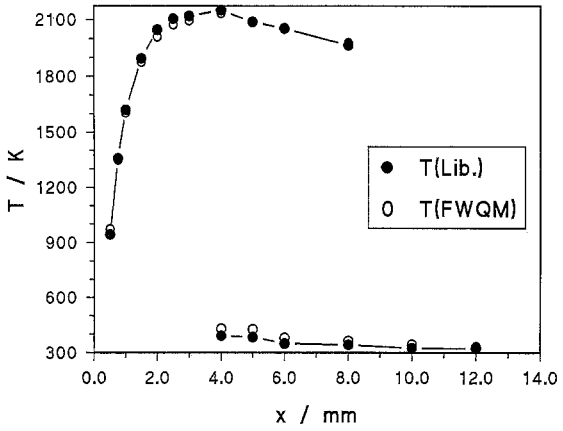

Fig. 4. Mean temperatures in the stagnation flame as a function of x. In regions with bimodal temperature distributions the low and high temperature values are displayed separately. The data points show the results of two different evaluation methods

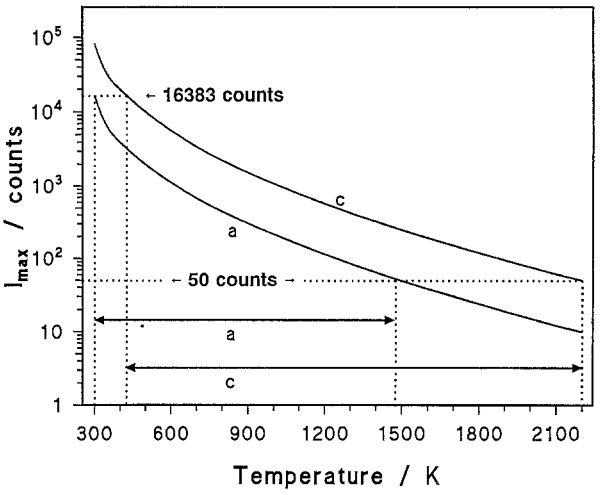

Fig. 5. Calculated peak intensities of CARS spectra as a function of temperature for two different laser powers. The effective dynamic range of the detector is limited to between 50 and 16383 counts

The temperatures in these histograms were evaluated by a quickfit method that derives the temperatures from the quarter-width (FWQM) of the CARS spectra. A more comprehensive library routine was also applied. A comparison of the results is shown in Fig. 4, which represents the development of the mean temperatures as a function of the distance x. The agreement between the results is excellent, and demonstrates that this quickfit method yields reliable temperature values.

A detailed examination of the accuracy was performed in the furnace experiment mentioned previously, and allows the uncertainties in our results to be specified. The mean temperatures are accurate to approximately $\pm 3\%$ and the spread-width of single pulse temperature values is about $\pm 5\%$.

5 Special Aspects and Problems

In order to measure temperatures in the turbulent reaction zone of a flame some modifications of the CARS technique had to be performed. The reasons for these modifications are due to some problems in detecting and analysing CARS spectra from regions with large temporal and spatial temperature fluctuations and with small turbulent structures. In the following sections these problems and our solutions are described in detail.

5.1 Dynamic Range of the Detector

The peak intensities of N_2 Q-branch CARS spectra from cold and hot gases vary by more than three orders of magnitude. The effective dynamic range of our intensified camera is approx. 300 if a minimum peak intensity of 50 counts is taken as necessary for a spectrum to be evaluated reliably. This means that temperatures of 300 and 2200 K cannot be measured under the same experimental conditions. Therefore, at locations with bimodal temperature distributions, two series of single pulse spectra with different laser powers were recorded: one with low laser power to detect the low temperature range, and another with high laser power for the upper temperature range. The situation is illustrated in Fig. 5 where the peak intensities I_{max} of CARS spectra, calculated for our experimental conditions, are displayed as a function of the temperature. Curve a represents the case for low laser powers with 16383 counts for cold gas of 300 K. The minimum peak intensity of 50 counts is reached at about 1470 K. Curve c is calculated for high laser powers with $I_{max} = 50$ counts for 2200 K. At this laser power all spectra with $T \leqq 420$ K saturate the detector. Under realistic experimental conditions these temperature limits are further reduced by statistical signal fluctuations due to laser beam perturbations in the turbulent reaction zone. However, there is still an overlapping range left between about 600 and 1300 K, where both series yield the same temperature distribution, thus allowing them to be fitted together at about 1000 K to obtain one complete temperature histogram.

The appropriate laser powers have to be chosen with great care, because too strong CARS signals, generated in cold gas by high laser powers, may damage the detector.

5.2 Image Persistence

It is well known that afterglow effects of intensified cameras can lead to a falsification of measured temperature values [8]. Measurements in our laboratory showed that the image persistence increases strongly by cooling the camera, whereas the dark current is reduced by cooling. Tolerating a rather high level of dark current, the detector was operated at a temperature of 15° C. Under these experimental conditions a CARS signal is superimposed on the detector by about 2% of the preceding signal pulse. In flame regions with large temperature fluctuations this amount cannot be neglected, especially if a strong (cold) CARS signal is followed by a weak (hot) one. By lowering the laser repetition rate in these regions

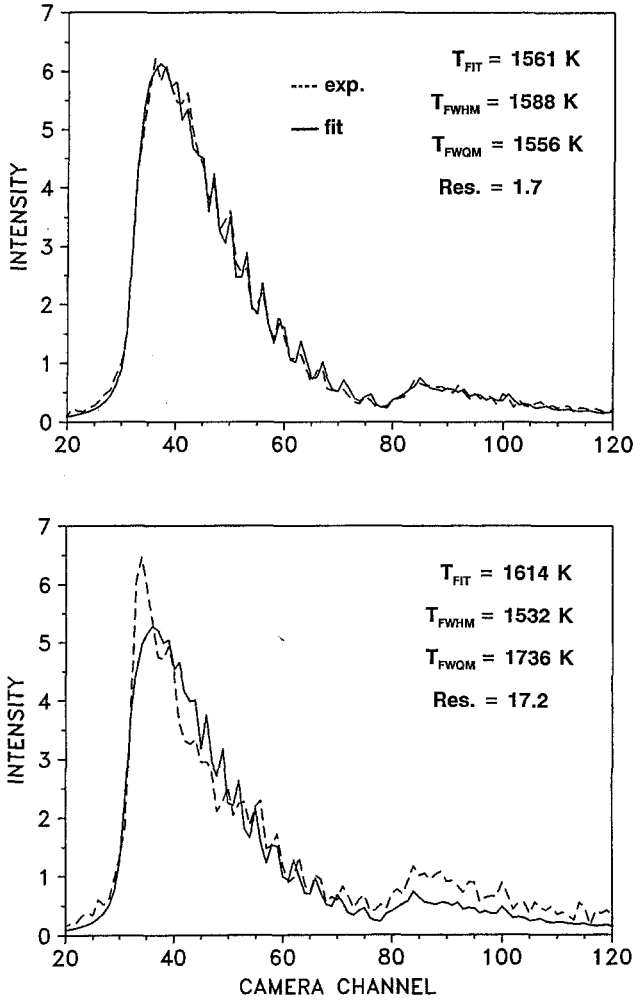

Fig. 6. Single pulse CARS spectra from a homogeneous and non-homogeneous temperature region in the flame. T_{Fit}, T_{FWHM}, and T_{FWQM} are the temperature values deduced from a least squares fit, the half-width of the spectrum, and the quarter-width, respectively. The comparison illustrates the effect of composite spectra

from 10 Hz to 2 Hz, the image persistence was reduced to an acceptable value of 0.3%.

In this context it should be mentioned that lasers with high repetition rates are of limited value for the investigation of turbulent flames as long as cameras with this drawback are used [18].

5.3 Spatial Resolution

Within the turbulent reaction zone the cold unburnt gas is separated from the hot burnt gas by a thin irregular flame front. It can occur that this flame front falls within the probe volume and that therefore some amount of cold and hot gases appear simultaneously in the probe volume, leading to composite CARS spectra without defined temperature. A reduction of the probe volume length could decrease the number of "mixed spectra" but at the same time it would lead to a significant loss in signal intensity as can be seen from (1). A compensation of this loss by higher laser powers is limited by the effect of Raman pumping. For that reason the spatial resolution for single shot CARS thermometry in turbulent flames cannot be made much better than 1–2 mm in length. Consequently, this problem has to be solved by an appropriate evaluation method. It seems to be almost impossible to deduce the exact temperature composition from a single pulse mixed CARS spectrum. On the other hand, the attempt to associate a "mean temperature" with mixed CARS spectra does not reflect the actual situation in the flame. For that reason the mixed spectra were identified by a screening method and rejected from further data evaluation. In order to explain and to justify the screening method, a comparison between a "pure" and a "mixed" single pulse CARS spectrum is shown in Fig. 6. The upper part shows a spectrum from a homogeneous temperature region. The agreement between the experimental data (dotted line) and the fitted spectrum (solid line) is excellent, and different evaluation methods lead to nearly the same temperature value. The spectrum in the lower part of Fig. 6 was recorded in a nonhomogeneous temperature region. Large discrepancies between the experimental and the fitted spectrum are apparent. In the spectral range up to about channel 40, which is attributed to low rotational quantum numbers of N_2, the shape is strongly influenced by cold gas contributions in the probe volume. Beyond channel 50, the hot gas contributes disproportionately strong to the spectral contour. The quantitative characteristics of such mixed spectra are large residual errors from least squares approximations and large deviations between different quickfit methods. In the given example the temperature value deduced from the half-width of the spectrum, T(FWHM), lies more than 200 K below the value that corresponds to the quarter-width, T(FWQM). This deviation between T(FWHM) and T(FWQM) is typical for mixed spectra.

To illustrate this behaviour, the differences T(FWHM) $-T$(FWQM) are shown in Fig. 7 for various locations within the flame. The results on the left hand side correspond to the exhaust region, in which the deviations are centred symmetrically around zero, with the spread-width increasing with temperature. The results from the turbulent flame region are presented on the right hand side of Fig. 7. In this case systematic deviations are obvious for a large number of data points: T(FWHM) lies significantly below T(FWQM). This effect is mainly due to mixed spectra, or in other words, to the limited spatial resolution.

This criterion is used to set up a screening method: all spectra with the temperature differences T(FWHM) $-T$(FWQM) beyond a certain limit were rejected. In Fig. 7 these limits are represented by the straight lines which correspond to the spread-width of the quickfit method T(FWHM), as determined in the furnace measurements, plus an additional offset of 15 K. The choice of the limits is somewhat arbitrary, and thus it is not completely possible to prevent some other spectra with large statistical variations from being filtered out, along with the undesired mixed spectra.

The influence of the screening process on a temperature histogram is illustrated in Fig. 8. The unhatched bars represent an unfiltered temperature distribution from the

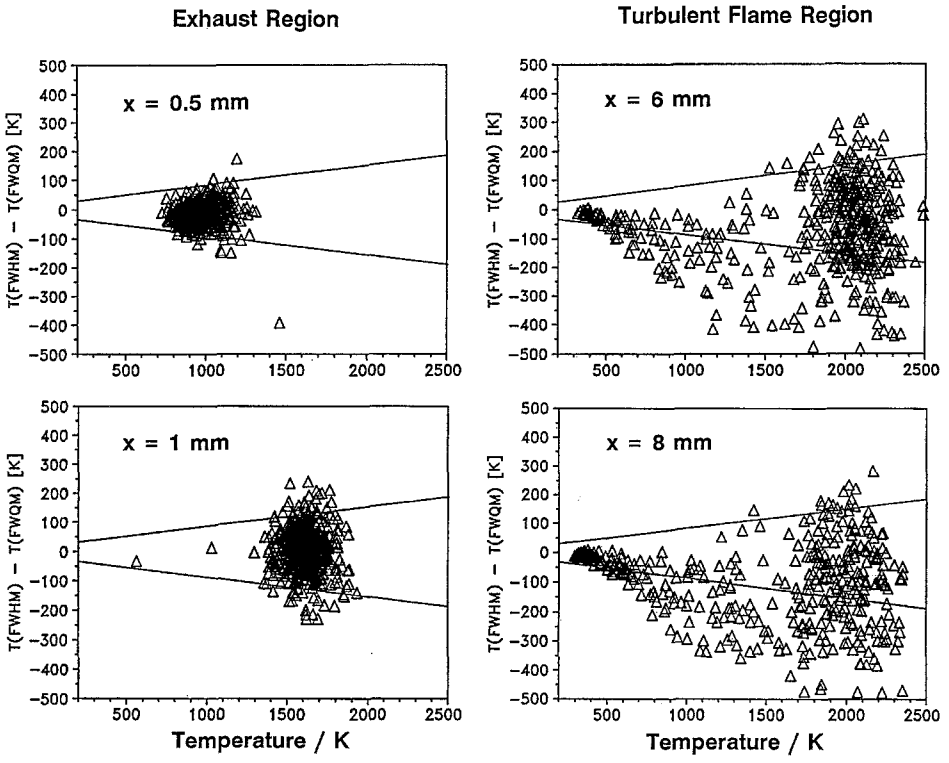

Fig. 7. Temperature deviations between the quickfit methods T(half-width) and T(quarter-width). The temperature on the horizontal axis is T(quarter-width). The influence of mixed CARS spectra from the turbulent flame region leads to systematic deviations. The straight lines represent the limits of the screening method

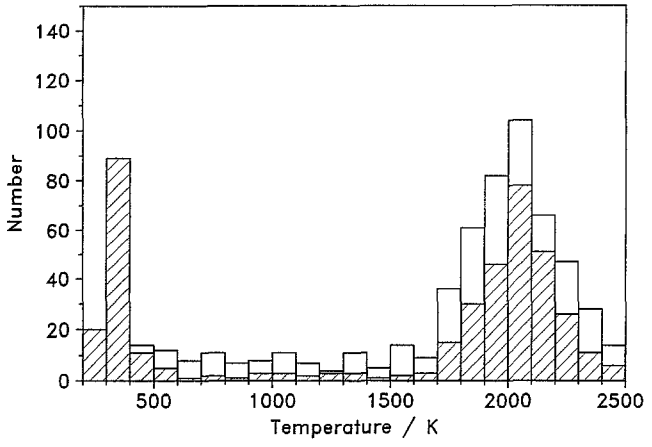

Fig. 8. Effect of screening on the temperature histograms. The unhatched and the hatched bars show the histogram before and after screening is applied

turbulent reaction zone, and the hatched bars show the result after screening. In the low temperature regime (200–500 K) almost no spectra are rejected, in the intermediate regime (600–1700 K) the majority of the spectra is filtered out, and in the upper temperature regime approximately every third one is rejected. This behaviour is quite reasonable, because of the bimodal nature of the turbulent combustion zone, intermediate temperature values should be scarce. The relative large number of filtered spectra in the upper temperature range is due to two effects: (1) The nonhomogeneous turbulent environment reduces the intensity and the quality of the spectra, leading to an increased spread-width of the involved quickfit methods. (2) A small percentage of cold gas in a mainly hot region can significantly change the shape of a spectrum, so that it is rejected by screening. The second effect is, again, a consequence of the fact that cold gas produces a much more intense CARS signal than hot gas. Accordingly, the screening results in a slight predominance of the cold parts (temperature biasing [3, 4]). This means the numerical ratio between the cold and hot parts of bimodal distributions can be shifted, although the mean temperatures and the width of each distribution remain unaffected. A detailed quantitative study of this effect is in progress.

The numbers by the side of the vertical axis in Fig. 3 indicate how many spectra contributed to the histograms after screening. At $x = 0.5$ mm, for example, 476 from 497 measured spectra are displayed in the histogram and 21 are rejected.

6 Discussion

Turbulent combustion zones with steep temperature gradients are a difficult and complicated area for single pulse CARS measurements. The described problems are well-known in CARS thermometry and have been discussed by several authors (e.g. [1, 3]). However, a summarizing description and a complete treatment under practical aspects is hard to find.

The problems are mainly based on the large intensity scale of the CARS signals from turbulent flames and on the small spatial structure in some types of turbulent reaction zones. These problems could, in principle, be solved by applying a detector with a larger dynamic range (to record hot and cold gases under the same experimental conditions without the risk of damage) and higher sensitivity (to allow a reduction of the probe volume size). But such devices are not so far available for the detection of single pulse spectra.

An insufficient spatial resolution can lead to a wrong interpretation of the measured data. Correctly determined temperature pdf's (probability density functions) give information about the structure of turbulent flame fronts. Depending on the turbulence intensity, different combustion regimes in premixed flames can be classified, ranging from laminar flames to well stirred reactions, as can be seen in the commonly used Borghi-diagram [19]. If the flame thickness is (infinitely) small, one would, theoretically (without spatial averaging), expect bimodal temperature pdf's within the turbulent flame where the two peaks correspond to the temperatures of burnt and unburnt gases. When the flame front becomes thicker, the probability for the occurrence of temperatures between the peaks increases, because within the flame front there exists an intermediate state between burnt and unburnt gas, where the temperature rises from the cold mixture to the hot exhaust gas. Finally, for distributed combustion (well stirred reactions) only small temporal and spatial temperature fluctuations occur [19]. In this way the temperature histograms include information about the flame structure, provided that they are not distorted by spatial averaging. For this reason it is important to distinguish between a "pure" CARS spectrum, with a well defined temperature, and a "composite" spectrum of a somehow averaged temperature. Under our flame conditions (Kolmogorov length ≈ 0.5 mm, laminar flame thickness ≈ 0.1 mm, integral length scale ≈ 6 mm) the flame front is not yet thickened but wrinkled, with pockets being possible. Therefore bimodal temperature pdf's would be expected within the flame front, with no or very little probability between the peaks.

Our main objective is the determination of temperature distributions and not the investigation of turbulence length scales. But as already shown, both quantities can be connected via the spatial resolution (not only in CARS thermometry), and therefore this is an important point for the determination and interpretation of temperature pdf's. However, it should be kept in mind that most technical combustion devices have bigger dimensions and larger turbulence length scales, and therefore a spatial resolution of 2 mm in length is sufficient for many applications.

Despite the discussed difficulties, the single pulse CARS technique seems to be the most suitable method for the determination of temperatures and temperature fluctuations in turbulent flames. By a proper choice of the experimental parameters and the application of appropriate evaluation routines, it is possible to determine reliable temperature distributions with high accuracy even in turbulent combustion zones.

Acknowledgements. This work was performed within the TECFLAM cooperative research program. The authors would like to thank B. Lenze and Y. Liu from Engler-Bunte-Institut, University of Karlsruhe, for the close cooperation in setting up the stagnation plate burner. The financial support by the Ministry of Research and Technology (BMFT) is gratefully acknowledged.

References

1. B. Attal-Trétout, P. Bouchardy, P. Magre, M. Péalat, J.P. Taran: Appl. Phys. B **51**, 17 (1990)
2. J.P. Boquillon, M. Péalat, P. Bouchardy, G. Collin, P. Magre, J.P. Taran: Opt. Lett. **13**, 722 (1988)
3. I.G. Shepherd, F.M. Porter, D.A. Greenhalgh: Combust. Flame **82**, 106 (1990)
4. P. Magre, P. Moreau, G. Collin, R. Borghi, M. Péalat: Combust. Flame **71**, 147 (1988)
5. R.J. Hall, A.C. Eckbreth: *Laser Applications*, Vol. V, ed. by J.F. Ready, R.K. Erf (Academic, New York 1984) p. 213
6. W.M. Tolles, J.W. Nibler, J.F. McDonald, A.B. Harvey: Appl. Spectrosc. **31**, 253 (1977)
7. D.A. Greenhalgh: Quantitative CARS Spectroscopy, in *Advances in Non-Linear Spectroscopy*, ed. by R.J.H. Clark, R.E. Hester (Wiley, London 1988) Chap. 5, p. 193
8. D.R. Snelling, G.J. Smallwood, T. Parameswaran: Appl. Opt. **28**, 3233 (1989)
9. Y. Liu, B. Lenze: The influence of turbulence on the laminar burning velocities of H_2–CH_4-mixtures. 22nd International Symposium on Combustion, Seattle (1988)
10. S. Kröll, M. Aldén, P.-E. Bengtsson, C. Löfström: Appl. Phys. B **49**, 445 (1989)
11. M. Woyde, W. Stricker: Appl. Phys. B **50**, 519 (1990)
12. M. Péalat, P. Bouchardy, M. Lefebvre, J.P. Taran: Appl. Opt. **24**, 1012 (1985)
13. R.J. Hall, L.R. Boedeker: Appl. Opt. **23**, 1340 (1984)
14. F. Porter: Ph. D. thesis, Surrey (1985)
15. A.C. Eckbreth, G.M. Dobbs, J.H. Stufflebeam, P.A. Tellex: Appl. Opt. **23**, 1328 (1984)
16. I. Plath: Ph. D. thesis, Stuttgart (1991)
17. Th. Dreier, B. Lange, J. Wolfrum, M. Zahn: Appl. Phys. B **45**, 183 (1988)
18. B. Lange, M. Noda, G. Marowsky: Appl. Phys. B **49**, 33 (1989)
19. R. Borghi: In *Recent Advances in the Aeronautical Sciences*, ed. by C. Bruno, C. Casci (Plenum, London 1985) p. 117